Macromolecules

pubs.acs.org/Macromolecules Article

Ultra-High-Molecular-Weight Macrocyclic Bottlebrushes via Post-Polymerization Modification of a Cyclic Polymer

Digvijayee Pal, Zhihui Miao, John B. Garrison, Adam S. Veige,* and Brent S. Sumerlin*

Cite This: *Macromolecules* 2020, 53, 9717−9724 Read Online

ACCESS | Metrics & More | Article Recommendations | Supporting Information

ABSTRACT: Polymer bottlebrushes are complex macromolecular nanostructures with polymeric side chains densely grafted to a polymer backbone. In this work, a synthetic strategy for the synthesis of cyclic bottlebrush polymers was exhibited by combining ring-expansion polymerization (REP) and atom transfer radical polymerization (ATRP) by a grafting-from approach. A variety of ultra-high-molecular-weight (on the order of MDa) macrocyclic bottlebrushes were generated by employing this method. Direct visualization of the macrocyclic bottlebrushes was achieved by atomic force microscopy. Furthermore, a linear bottlebrush polymer was synthesized independently by a similar synthetic route to investigate topological differences between cyclic and linear architectures.

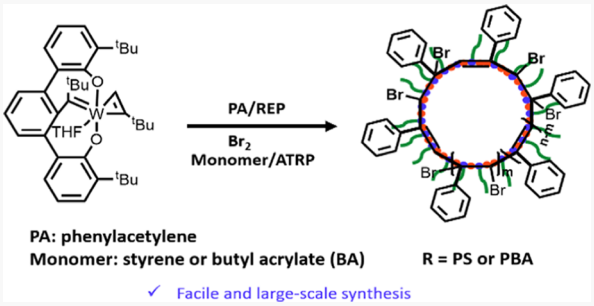

Advances in synthetic polymer chemistry have enabled access to macromolecules with complex topologies, including, for example, macrocycles, bottlebrushes, stars, and dendronized, hyperbranched, figure 8 or theta-shaped chains.[1−8] The generation of cyclic topologies is of particular interest as their solution and bulk properties differ from those of linear polymers of similar molecular weights.[9−17]

Bottlebrush polymers have been integral in many developing fields including drug delivery systems, lubricating materials, and elastomeric gels. Cyclic bottlebrushes, on the other hand, have not been explored to this extent due, in part, to limitations in purity and synthetic challenges presented during their preparation. Ring-closing techniques of α- and ω-end groups to form cyclic polymers generate unavoidable linear impurities from competing intermolecular coupling.[14,15] Excitingly, recent developments in ring-expansion polymerization (REP) with ruthenium or tungsten-based catalysts enable the synthesis of pure cyclic polymers with excellent yields (>98%).[13,18−26]

The generation of bottlebrushes from a cyclic backbone can be accomplished by three different techniques.[27] The first is the grafting-to approach, which involves attaching independently synthesized side chains to a cyclic backbone via highly efficient reactions, such as Cu-catalyzed azide-alkyne cycloaddition (CuAAC), thiol-Michael addition, and Diels−Alder reactions.[28−31] In 2008, Schappacher and Deffieux[29] reported a synthetic route in which they first synthesized an ABC triblock polymer with chloroethyl vinyl ether as the B block. Connecting A and C block ends under highly dilute conditions generated a cyclic polymer. Subsequently, attaching polystyrene (PS), polyisoprene, and polystyrene/polyisoprene side chains to the cyclic backbone produced macrocyclic brushes. Gel permeation chromatography (GPC) and atomic force microscopy (AFM) characterizations of the brushes confirmed their cyclic topology.

Grafting-through, a second approach for generating a cyclic bottlebrush polymer, generally involves polymerization of macromonomers using tethered metal catalysts.[32,33] In 2011, Grubbs and co-workers[33] generated macrocyclic brushes of ultrahigh molecular weights by polymerizing ω-norbornenyl macromonomers with polystyrene and poly(lactic acid) side chains using tethered ruthenium alkylidene catalysts. The cyclic brushes had molecular weights on the order of MDa. AFM analysis revealed donut-shaped structures with diameters smaller than that of the theoretical diameters predicted for fully extended backbones, as well as some linear brush impurities. It is noteworthy that the rings underwent scission 2 h after deposition on the mica surface due to high mechanical strain on the backbones, a phenomenon reported by Matyjaszewski, Sheiko, and co-workers in the case of linear bottlebrush polymers as well.[34,35]

A third route to generating side chains on a macrocyclic polymer backbone is a grafting-from approach, where side chains are grown from the backbone. This approach is often accomplished via reversible-deactivation radical polymerization (RDRP) techniques, such as atom transfer radical polymer-

Received: August 3, 2020
Revised: September 23, 2020
Published: November 4, 2020

https://dx.doi.org/10.1021/acs.macromol.0c01797
Macromolecules 2020, 53, 9717−9724

Scheme 1. Synthesis of Cyclic Bottlebrush Polymers with Polystyrene and Poly(butyl acrylate) Side Chains

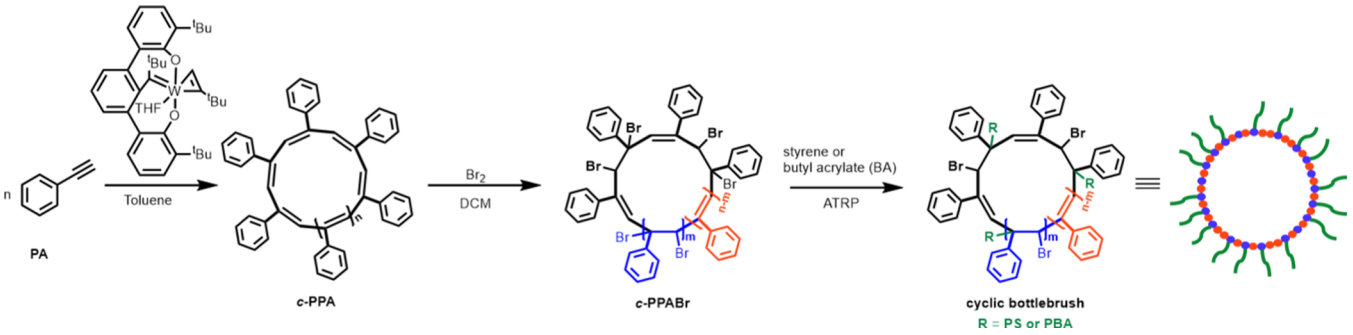

ization (ATRP) and reversible addition-fragmentation chain transfer polymerization (RAFT), or, alternatively, by ring-opening polymerization (ROP).[36−42] Zhang and Tew[36] synthesized a polynorbornene-based cyclic backbone with hydroxyl group-containing repeat units. Performing triazabicyclodecene-catalyzed ring-opening polymerization of cyclic esters to grow ester side chains from the hydroxyl groups ultimately produced cyclic brushes.

The grafting-from approach possesses some advantages over the grafting-to and grafting-through approaches, as pure cyclic brushes with high grafting density are difficult to achieve by the latter techniques. Zhu and co-workers[40] synthesized a variety of macrocyclic brushes using ATRP and a grafting-from approach with a universal cyclic polystyrene template. A low-molecular-weight (around 5 kDa) polystyrene backbone was utilized to perform macrocyclization via CuAAC. High-molecular-weight brushes were generated from the macroinitiators, though bimodal GPC traces indicated the presence of some impurities. Pun and co-workers[41] also reported a "sunflower polymer" by exploiting ATRP and a grafting-from technique for a tumor-targeted drug delivery application. Several other studies have suggested that the drug delivery capability of cyclic brush polymers surpasses that of their linear analogs.[37−39,42]

Encouraged by these advances, we developed a straightforward synthetic strategy for the formation of cyclic bottlebrushes with PS and poly(butyl acrylate) (PBA) side chains from a cyclic polyphenylacetylene (PPA) precursor by combining REP and a subsequent grafting-from approach with ATRP. Characterization via GPC with static light scattering (SLS) and viscometric detection provided evidence for the cyclic topology of the polymer precursor prior to grafting. ^{1}H NMR spectroscopy and GPC analysis provided confirmation of the formation of ultra-high-molecular-weight cyclic bottlebrushes, while direct visualization with AFM was consistent with the presence of circular topologies. Furthermore, a linear bottlebrush polymer with PS side chains was synthesized independently to investigate differences in polymer properties induced by the topological differences between cyclic and linear bottlebrushes.

RESULTS AND DISCUSSION

Phenylacetylene was polymerized via REP with a tetra-anionic pincer ligand-supported tungsten catalyst[18,43] at ambient temperature to produce cyclic PPA (***c*-PPA**) in >99% yield (Scheme 1). ^{1}H NMR spectroscopic analysis of the product exhibited the expected characteristic proton resonances (Figure S1). GPC analysis of the purified cyclic polymer revealed a monomodal molecular weight distribution with a number-average molecular weight (M_n) of 330 kDa and a dispersity (M_w/M_n) of 1.38 (Figure S2). To aid in comparing the cyclic architecture to a linear counterpart, linear PPA (***l*-PPA**) was also synthesized using acetylacetonato(1,5-cyclooctadiene) rhodium(I) as the catalyst in THF at ambient temperature.[44,45] The resulting linear polymer was characterized by ^{1}H NMR spectroscopy (Figure S3) and GPC (M_n = 213 kDa and M_w/M_n = 1.68) (Figure S4). Evidence of the cyclic topology for the polymer prepared with the tungsten catalyst was obtained by two characteristic GPC plots.[13,18,24,25,46] When comparing the plot of log(molar mass) versus elution time for ***c*-PPA** and ***l*-PPA** (Figure 1A),

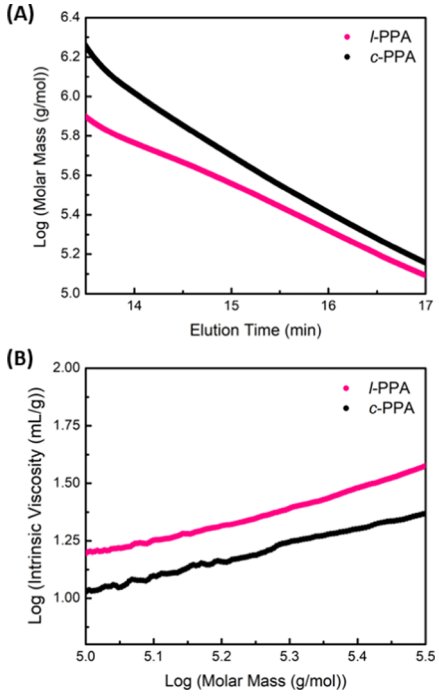

Figure 1. (A) Log(molar mass) versus elution time plot of cyclic (black line) and linear (pink line) polyphenylacetylene (**PPA**). (B) Log(intrinsic viscosity) versus log(molar mass) plot of cyclic (black line) and linear (pink line) PPA.

it was clear that at any point along the elugram that ***c*-PPA** eluted later than its linear counterpart of identical molecular weight. Moreover, the plot of log(intrinsic viscosity) versus log(molar mass) (Figure 1B) indicated a consistently lower intrinsic viscosity of ***c*-PPA** compared to its linear analog at a given molecular weight. These data are consistent with the

https://dx.doi.org/10.1021/acs.macromol.0c01797
Macromolecules 2020, 53, 9717−9724

Scheme 2. Synthesis of a Linear Bottlebrush Polymer with Polystyrene Side Chains

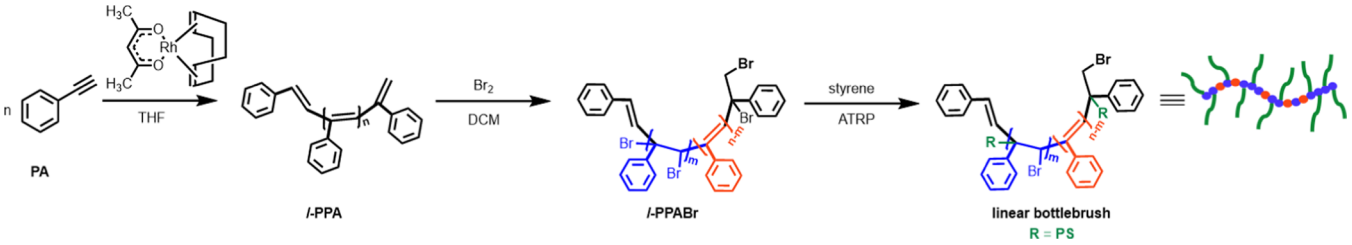

Table 1. Synthesis of Cyclic and Linear Bottlebrush Polymers Using Brominated Cyclic and Linear Macroinitiators

entry[a]	[monomer]:[macroinitiator][b]	time (h)	conversion[c] (%)	$M_{n,theo}$[d] (kDa)	$M_{n,GPC}$[e] (kDa)	M_w/M_n
			linear			
l-PPABr				453	345	1.65
bottlebrush	100:1	72	32	5760	5560	1.71
			cyclic			
c-PPABr				437	411	1.41
CB-PS-1a	25:1	48	12	820	755	1.41
CB-PS-1b	50:1	48	15	1390	1340	1.36
CB-PS-1c	100:1	48	22	3250	3670	1.35
CB-PS-1d	200:1	112	38	9880	8760	1.21
CB-PBA-1a	50:1	36	12	1200	1150	1.36
CB-PBA-1b	100:1	36	18	2730	2340	1.39
CB-PBA-1c	200:1	36	26	7070	6580	1.37

[a]CB = cyclic bottlebrush; PS = polystyrene; and PBA = poly(butyl acrylate). [b]Molar ratio of monomer to macroinitiator. [c]Monomer conversions were calculated via ^{1}H NMR analysis using trioxane as an internal standard. [d]Theoretical number-average molecular weight of the brushes. [e]Absolute number-average molecular weight determined by gel permeation chromatography (GPC) equipped with a multiangle light scattering detector and using DMAc as a mobile phase at 50 °C; d*n*/d*c* values required to calculate molecular weights were obtained by assuming 100% mass-recovery during elution.

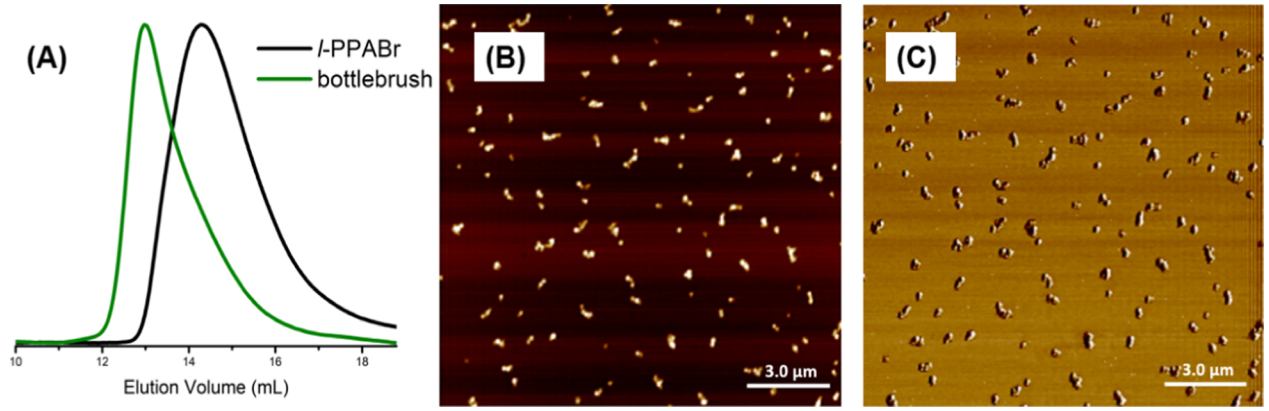

Figure 2. (A) GPC traces of the linear macroinitiator and the linear bottlebrush polymer exhibiting a monomodal shift to lower elution volume, i.e., toward higher molecular weights. AFM height (B) and phase (C) images of the linear bottlebrush polymer.

cyclic architecture of ***c*-PPA** leading to a decrease in hydrodynamic volume and solution viscosity.

To generate macroinitiators with initiation sites along the cyclic and linear backbones, ***c*-PPA** (Scheme 1) and ***l*-PPA** (Scheme 2) were brominated via the electrophilic addition of Br_2. The benzylic positions of the resulting polymers were expected to be susceptible to grafting-from polymerization via ATRP. ^{1}H NMR analysis was insufficient to determine the bromine incorporation efficiency, as the methine signals overlapped with those from the aromatic protons (Figures S5 and S6). Even with high-temperature ^{1}H NMR analysis at 100 °C of the brominated ***c*-PPA** (***c*-PPABr**), it was not possible to determine the extent of bromination. However, the elemental analysis revealed that the fraction of double bonds brominated in the ***c*-PPABr** and ***l*-PPABr** were 52 and 72%, respectively. Using lower equivalents of bromine led to lower bromine incorporation in the cyclic PPA (Table S3). However, the addition of greater than five equivalents of bromine per repeat unit resulted in backbone degradation. M_n and M_w/M_n of ***l*-PPABr** and ***c*-PPABr** used in the subsequent grafting-from polymerizations are given in Table 1.

Scheme 2 depicts the synthesis of the linear bottlebrush polymer with polystyrene side chains grafted from the linear macroinitiator ***l*-PPABr**. Typical ATRP conditions using copper bromide (CuBr) as a catalyst, 1,1,4,7,7-pentamethyl diethylenetriamine (PMDETA) as a ligand, and styrene to macroinitiator ratio of 100:1 were employed. Polymerization was deliberately quenched at 32% monomer conversion after

https://dx.doi.org/10.1021/acs.macromol.0c01797
Macromolecules 2020, 53, 9717−9724

72 h to avoid cross-coupling between the side chains. ^{1}H NMR analysis of the resulting polymer showed characteristic polystyrene protons (Figure S7). GPC analysis showed that the M_n of the linear bottlebrush polymer increased from 345 to 5560 kDa after grafting. GPC traces (Figure 2A) exhibited a monomodal shift toward higher molecular weights with dispersity similar to that of the macroinitiator, a common phenomenon observed in the case of linear bottlebrush polymers.[47]

Gradual shifts of RI signals toward lower elution time with increasing reaction time were observed (Figure S8), suggesting high-molecular-weight bottlebrush polymers were being formed. Reaction rate analysis showed that monomer consumption followed linear pseudo-first-order kinetics throughout the polymerization (Figure S9), suggesting the presence of a constant radical flux during the polymerization. Additionally, a linear growth of M_n with monomer conversion was observed, indicating the absence of any significant chain transfer processes (Figure S10). These results are consistent with a controlled ATRP grafting reaction and the efficacy of benzylic bromine positions on ***l*-PPABr** as initiating sites.

AFM analysis of a highly dilute (1 μg/mL) solution of the linear bottlebrushes in tetrahydrofuran (THF) spin-coated on a mica surface provided visualization of the topology of these polymers. Figures 2B and C depict a height and a phase image, respectively. The length of the bottlebrushes varied from 330 to 590 nm. This variability in size is not surprising given the relatively high dispersity of the macroinitiator. The theoretical length of the polymer along the backbone was 400 nm (Table S4), calculated based on the $M_{n,GPC}$ of the polymer backbone and side chains, and assuming each repeat unit is of 0.252 nm[47,48] in length (Calculation S1). It is interesting to note that the shape of the linear bottlebrushes is not perfectly cylindrical as reported previously.[48] We hypothesize that due to partial bromination, ~28% of the double bonds remain along the backbone resulting in lower grafting density. Consequently, the brushes are not expected to be fully extended along their backbones.

Encouraged by the success in synthesizing linear bottlebrushes from the linear macroinitiator, initially, we attempted to synthesize macrocyclic bottlebrushes with polystyrene side chains using the macroinitiator ***c*-PPABr**. Employing typical ATRP conditions with CuBr as a catalyst, PMDETA as a ligand, and styrene as the monomer, polystyrene side chains of different chain lengths were grafted from the macroinitiator. ^{1}H NMR analysis of the resulting polymers exhibited only the characteristic polystyrene protons without any backbone protons (Figure S11), consistent with the fact that most of the polymer being composed of the polystyrene side chains that obscure the backbone signals. Additionally, the ^{13}C NMR spectra of ***c*-PPABr** and **CB-PS-1c** (Figure S12) revealed a complete disappearance of the C-Br peak at ~68 ppm. Only the characteristic polystyrene carbon peaks were observed without any backbone alkene and phenyl carbons being visible, consistent with the fact that the newly grown polystyrene side chains overwhelm and obscure the backbone signals.

Table 1 depicts molecular weights and M_w/M_n of the cyclic bottlebrushes synthesized with varying styrene to ***c*-PPABr** ratios. Brushes with increasing molecular weight from 755 to 4120 kDa were observed with increasing molar ratios of monomer to macroinitiator from 25:1 to 100:1 (Figure 3). Additionally, $M_{n,GPC}$ for each brush showed good agreement with the theoretical M_n calculated based on the stoichiometry

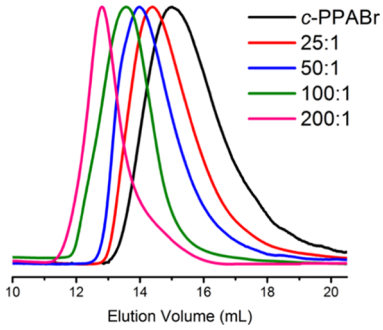

Figure 3. GPC traces of cyclic bottlebrushes with polystyrene side chains prepared at different styrene to macroinitiator molar ratios.

and monomer conversions. Dispersity of the resulting brushes remained almost equivalent to that of the macroinitiator, which is in good agreement with the phenomenon expected for any brush polymer prepared by a grafting-from approach.[47]

A kinetic study on the polymerization used to prepare **CB-PS-1c** (100:1 styrene to macroinitiator molar ratio) revealed monomodal shifts of RI traces toward higher molecular weights with increasing reaction times (Figure S13), while dispersity remained relatively constant throughout the polymerization, with the exception for the brush of 7260 kDa obtained at 47% styrene conversion. This sample being of exceptionally high M_n eluted near the void volume of the GPC column set,[4950] which could suggest that this sample was not adequately fractionated, potentially accounting for the discrepancy in M_w/M_n. This hypothesis could also be applied to the exceptionally high-molecular-weight polymer **CB-PS-1d** that showed a lower dispersity than ***c*-PPABr** (Table 1). The controlled nature of the ATRP grafting reaction was evidenced by a pseudo-first-order kinetic plot, which also indicated a constant radical concentration during the polymerization (Figure 4). Linear growth of M_n with monomer conversion suggests efficient initiation[47] and negligible chain transfer reactions (Figure 5).

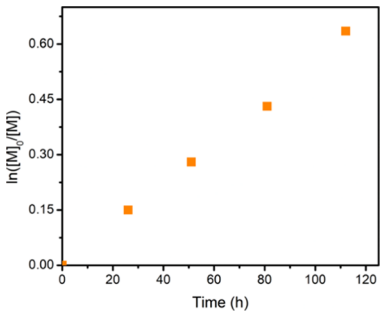

Figure 4. Pseudo-first-order kinetic plot of the cyclic bottlebrush polymer **CB-PS-1c** (100:1 styrene to macroinitiator molar ratio).

AFM analysis of **CB-PS-1a** revealed ring-shaped structures when a highly dilute solution of the polymer in THF (1 μg/mL) was spin-coated on a mica surface (Figure S14). The circular shapes are consistent with the cyclic topology of the macrocyclic bottlebrushes[51] expected for backbone synthesis via REP of acetylenic monomers. The outer diameters of the circular structures range from 25 to 50 nm, which are well below the theoretical outer diameter of ~180 nm (Table S4), calculated based on the $M_{n,GPC}$ of the backbone and side chains and assuming a fully extended backbone. A thorough

https://dx.doi.org/10.1021/acs.macromol.0c01797
Macromolecules 2020, 53, 9717−9724

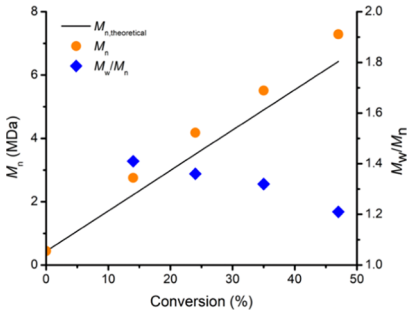

Figure 5. M_n and M_w/M_n plot as a function of monomer conversion of the cyclic bottlebrush polymer **CB-PS-1c** (100:1 styrene to macroinitiator molar ratio).

calculation of the theoretical dimensions of the polymer was reported in the Supporting Information (see Calculation S2). The smaller diameter could be attributed to the relatively short side chain length of polystyrene [average degree of polymerization (DP_n = 3)] and the fact that not every unit of the backbone was susceptible to grafting-from, which leads to less than full backbone extension or to weak polystyrene−surface interactions. These sorts of exceptionally low actual diameters of cyclic bottlebrushes were also reported by Grubbs and co-workers,[33] where donut-shaped structures with diameters of ca. 35−40 nm were observed, even with a polymer of M_n of 5.26 MDa and a DP_n as high as 5840. Nonetheless, the presence of a depression in the middle of the brush architecture was clearly identified, which is consistent with the anticipated cyclic topology. The cross-sectional analysis (Figure S14) of the height traces was also consistent with the successful synthesis of the cyclic bottlebrushes. Additionally, AFM analysis on **CB-PS-1b** (50:1, styrene to macroinitiator molar ratio) also produced ring-shaped structures with outer diameters in the range of 40−55 nm (Figure S15).

When the styrene to macroinitiator molar ratio is increased from 25:1 to 200:1, in the case of **CB-PS-1d**, the side chain length of the brushes increased from ∼1 to ∼18 nm, calculated based on the theoretical DP_n of 70 for the side chains, and assuming a length of each repeat unit of 0.252 nm (Table S4). The theoretical outer diameter of this polymer at a fully extended conformation is 196 nm (Table S4), calculated based on the $M_{n,GPC}$ of the polymer (see the sample Calculation S2). AFM analysis on these cyclic bottlebrushes once again exhibited clear ringlike structures with the outer diameters ranging from 120 to 200 nm (Figure 6A−C), almost matching the theoretical diameters. This observation indicates that longer side chains can induce higher backbone stretching, a phenomenon well established in the case of linear bottlebrush polymers.[48] Moreover, the presence of a depression in the observed polymers' topology was more pronounced in this case, as confirmed from the cross-sectional analysis on the AFM height profile (Figure S16). Some wormlike structures were also visible in the AFM images. It might be possible that the spin-coating process generates high mechanical strain on the backbones of the cyclic bottlebrush polymers, resulting in some objects that appear to be linear bottlebrush polymers. Matyjaszewski,[34] Sheiko, and co-workers[35] have found that high-molecular-weight, densely grafted linear bottlebrush polymers are prone to rapid mechanical degradation through backbone scission. They attributed this phenomenon to concentrated tension on the backbone due to adsorption of high density, long side chains at surfaces. Grubbs and co-workers[32] also observed this phenomenon for their ultra-high-molecular-weight cyclic brush polymers and hypothesized that the polymers may have been even more susceptible to cleavage considering the additional stress in the backbone from the forced curving.

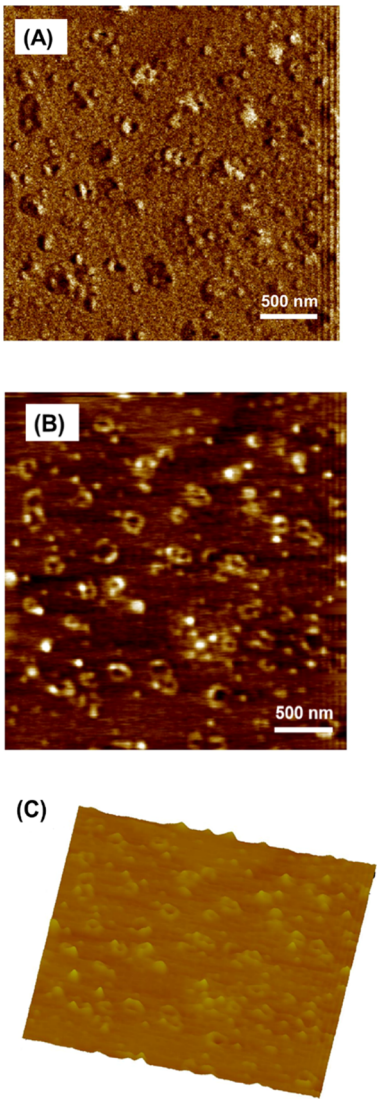

Figure 6. AFM phase (A), height (B), and three-dimensional (C) images of **CB-PS-1d** (obtained from a 200:1 styrene to macroinitiator molar ratio), showing a circular topology of the polymer.

To expand the diversity of macrocyclic bottlebrushes prepared by this tandem REP-ATRP approach, the next aim was to generate a cyclic bottlebrush polymer with poly(butyl acrylate) side chains. In this case, three different butyl acrylate to ***c*-PPABr** ratios were employed, specifically 50:1, 100:1, and 200:1, to synthesize **CB-PBA-1a**, **CB-PBA-1b**, and **CB-PBA-1c**, respectively (Table 1). Examination of the ^{1}H NMR and ^{13}C NMR spectra of **CB-PBA-1a** revealed broad signals from ∼5.5 to 7 ppm in the ^{1}H NMR spectrum (Figure S17) and from ∼125 to 135 ppm in the ^{13}C NMR spectrum (Figure S18) that were nearly obscured by the baseline. These small resonances are attributable to backbone alkene and phenyl protons within the polymer structure. In contrast, ^{1}H NMR analysis of both the **CB-PBA-1b** and **CB-PBA-1c** polymers showed only the characteristic −**OC*H*$_2$**− resonances at 4.0 ppm (Figure S19), with the ring polymer backbone protons

https://dx.doi.org/10.1021/acs.macromol.0c01797
Macromolecules 2020, 53, 9717−9724

being obscured by the PBA side chains. Additionally, the ^{13}C NMR spectrum of ***c*-PPABr** and **CB-PBA-1a** (Figure S12) revealed a complete disappearance of the C-Br resonance at ~68 ppm. Only the characteristic PBA carbon signals were observed without any backbone alkene and phenyl carbons being visible, consistent with the fact that the newly grown PBA side chains overwhelm and obscure the backbone signals. Initially, we used a CuBr/PMDETA for the ATRP synthesis of the side chains via a grafting-from approach. Unfortunately, adding PMDETA as a ligand produced brush polymers with a bimodal distribution, as determined by GPC analysis. We hypothesized that due to low deactivation in the presence of a highly active catalyst/ligand system, some of the benzylic brominated sites of the macroinitiators remained uninitiated. Employing the less reactive ligand [i.e., 4,4′-dinonyl-2,2′-dipyridyl (dNbpy)],[47,48] macrocyclic brushes with monomodal distributions were obtained. The M_n of **CB-PBA-1a**, **CB-PBA-1b**, and **CB-PBA-1c** increased from that of the macroinitiator ***c*-PPABr** after grafting, from 411 to 1150, 2340, and 6580 kDa with dispersities of 1.36, 1.39, and 1.37, respectively (Table 1, Figure 7A).

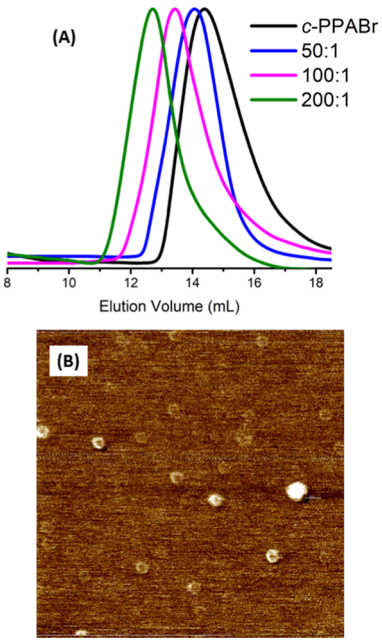

Figure 7. (A) GPC traces of cyclic bottlebrushes with poly(butyl acrylate) side chains prepared at different butyl acrylate to macroinitiator molar ratios. (B) AFM phase image of **CB-PBA-1b** (100:1 butyl acrylate to macroinitiator ratio).

Once again, AFM analysis of the macrocyclic bottlebrushes after spin-coating from a dilute THF solution (1 μg/mL) on a mica surface provided information about the topology of the brushes. **CB-PBA-1b** exhibited circular structures with an outer diameter of 25−50 nm (Figure 7B). The cross-sectional analysis of the height traces was also indicative of the successful synthesis of cyclic bottlebrushes (Figure S20). Again, the outer diameter of the brushes was well below the theoretical diameter (182 nm) expected for cyclic bottlebrushes with fully extended backbones. The theoretical diameter was calculated based on the $M_{n,GPC}$ of the backbone and side chains (Table S4). These results are again consistent with the backbones being less than fully extended in the presence of short side chains length with lengths of only ~4 nm and a relatively low grafting density. This phenomenon was also observed by Grubbs and co-workers[33] for cyclic polynorbornene brush polymers. AFM analysis of **CB-PBA-1c** also revealed circular structures with diameters ~70−80 nm, higher than that of **CB-PBA-1b**, presumably due to the relatively longer side chain length of 13 nm (Figure S21).

CONCLUSIONS

Cyclic bottlebrushes were generated from cyclic PPA precursors. Controlled grafting-from polymerization of side chains from both linear and cyclic macroinitiators was achieved with ATRP. The versatility of this approach was illustrated by grafting polystyrene and poly(butyl acrylate) from the cyclic macroinitiator of different side chain lengths. Direct imaging by AFM confirmed the cyclic topology of the brushes. Increasing the side chain lengths resulted in an enhancement of the outer diameter of the polymers, leading to a clear visual depression in the center of the polymers' architecture. Linear bottlebrush polymers with polystyrene side chains were also synthesized to further examine the topological differences between the cyclic and linear bottlebrushes.

This unique approach of integrating REP and ATRP can be applied to generate a variety of macrocyclic bottlebrushes with different functionalities for targeted applications. It is well documented that materials with supersoft and superelastic qualities[52,53] can be formed by cross-linking linear bottlebrush polymers. Cyclic bottlebrushes offer an opportunity to expand the range of possible properties for these materials. Therefore, the future focus will be to explore the differences between cross-linked examples of cyclic and linear bottlebrushes prepared by this tandem REP-ATRP approach.

Confirming a cyclic topology for cyclic polymers and producing them on a large scale is challenging. Though strong supporting evidence from size exclusion chromatography, dynamic light scattering, static light scattering, intrinsic viscosity, ozonolysis, and rheology clearly support a cyclic topology for polymers produced using our W-catalyst,[18,24,25] absolute evidence for the topology was missing. The AFM images presented herein for two different cyclic bottlebrushes and their size relationship with DP_n, provide for the first time, absolute evidence for a cyclic topology. Finally, the large-scale synthesis of the macroinitiator enables cyclic bottlebrushes to be synthesized on gram scales, which will be important if the exciting topological properties of cyclic bottlebrush polymers are to be exploited in the future.

ASSOCIATED CONTENT

Supporting Information

The Supporting Information is available free of charge at https://pubs.acs.org/doi/10.1021/acs.macromol.0c01797.

Full experimental procedures, NMR spectra, GPC data, and AFM data (PDF)

AUTHOR INFORMATION

Corresponding Authors

Adam S. Veige − *George & Josephine Butler Polymer Research Laboratory, Center for Macromolecular Science & Engineering, Department of Chemistry and Center for Catalysis, Department of Chemistry, University of Florida, Gainesville, Florida 32611, United States;* orcid.org/0000-0002-7020-9251; Email: veige@chem.ufl.edu

https://dx.doi.org/10.1021/acs.macromol.0c01797
Macromolecules 2020, 53, 9717−9724

Brent S. Sumerlin − *George & Josephine Butler Polymer Research Laboratory, Center for Macromolecular Science & Engineering, Department of Chemistry, University of Florida, Gainesville, Florida 32611, United States;* orcid.org/0000-0001-5749-5444; Email: sumerlin@chem.ufl.edu

Authors

Digvijayee Pal − *George & Josephine Butler Polymer Research Laboratory, Center for Macromolecular Science & Engineering, Department of Chemistry, University of Florida, Gainesville, Florida 32611, United States*

Zhihui Miao − *George & Josephine Butler Polymer Research Laboratory, Center for Macromolecular Science & Engineering, Department of Chemistry and Center for Catalysis, Department of Chemistry, University of Florida, Gainesville, Florida 32611, United States*

John B. Garrison − *George & Josephine Butler Polymer Research Laboratory, Center for Macromolecular Science & Engineering, Department of Chemistry, University of Florida, Gainesville, Florida 32611, United States*

Complete contact information is available at: https://pubs.acs.org/10.1021/acs.macromol.0c01797

Notes

The authors declare no competing financial interest.

■ ACKNOWLEDGMENTS

This material is based upon work supported by the National Science Foundation (CHE-1808234).

■ REFERENCES

(1) Matyjaszewski, K.; Xia, J. Atom transfer radical polymerization. *Chem. Rev.* **2001**, *101*, 2921−2990.
(2) Kamigaito, M.; Ando, T.; Sawamoto, M. Metal-catalyzed living radical polymerization. *Chem. Rev.* **2001**, *101*, 3689−3746.
(3) Tezuka, Y. *Topological Polymer Chemistry: Progress of Cyclic Polymers in Syntheses, Properties, and Functions*; World Scientific, 2013.
(4) Schluter, A. D.; Rabe, J. P. Dendronized polymers: synthesis, characterization, assembly at interfaces, and manipulation. *Angew. Chem., Int. Ed.* **2000**, *39*, 864−883.
(5) Sims, M. B.; Patel, K. Y.; Bhatta, M.; Mukherjee, S.; Sumerlin, B. S. Functional diversification of polymethacrylates by dynamic β-ketoester modification. *Macromolecules* **2018**, *51*, 356−363.
(6) Pangilinan, K.; Advincula, R. Cyclic polymers and catenanes by atom transfer radical polymerization (ATRP). *Polym. Int.* **2014**, *63*, 803−813.
(7) Gao, H.; Tsarevsky, N. V.; Matyjaszewski, K. Synthesis of degradable miktoarm star copolymers via atom transfer radical polymerization. *Macromolecules* **2005**, *38*, 5995−6004.
(8) Sumerlin, B. S.; Matyjaszewski, K. *Molecular Brushes-Densely Grafted Copolymers in Macromolecular Engineering*; Matyjaszewski, K.; Gnanou, Y.; Leibler, L., Eds.; Wiley-VCH: Weinheim, 2007; Vol. 2, pp 1103−1135.
(9) Bloomfield, V.; Zimm, B. H. Viscosity, sedimentation, et cetera, of ring- and straight-chain polymers in dilute solution. *J. Chem. Phys.* **1966**, *44*, 315−323.
(10) Roovers, J. Dilute-solution properties of ring polystyrenes. *J. Polym. Sci., Part B: Polym. Phys.* **1985**, *23*, 1117−1126.
(11) García Bernal, J. M.; Tirado, M. M.; Freire, J. J.; Garcia de La Torre, J. Monte Carlo calculation of hydrodynamic properties of linear and cyclic polymers in good solvents. *Macromolecules* **1991**, *24*, 593−598.
(12) Zimm, B. H.; Stockmayer, W. H. The dimensions of chain molecules containing branches and rings. *J. Chem. Phys.* **1949**, *17*, 1301−1314.
(13) Bielawski, C. W.; Benitez, D.; Grubbs, R. H. An "endless" route to cyclic polymers. *Science* **2002**, *297*, 2041−2044.
(14) Liénard, R.; Winter, J. D.; Coulembier, O. Cyclic polymers: Advances in their synthesis, properties, and biomedical applications. *J. Polym. Sci.* **2020**, *58*, 1481−1502.
(15) Haque, F. M.; Grayson, S. The synthesis, properties and potential applications of cyclic polymers. *Nat. Chem.* **2020**, *12*, 433−444.
(16) Laurent, B. A.; Grayson, S. M. Synthetic approaches for the preparation of cyclic polymers. *Chem. Soc. Rev.* **2009**, *38*, 2202.
(17) Touris, A.; Hadjichristidis, N. Cyclic and multiblock polystyrene-block-polyisoprene copolymers by combining anionic polymerization and azide/alkyne "click" chemistry. *Macromolecules* **2011**, *44*, 1969−1976.
(18) (a) Roland, C. D.; Li, H.; Abboud, K. A.; Wagener, K. B.; Veige, A. S. Cyclic polymers from alkynes. *Nat. Chem.* **2016**, *8*, 791−796. (b) Roland, C. D.; Zhang, T.; VenkatRamani, S.; Ghiviriga, I.; Veige, A. S. A catalytically relevant intermediate in the synthesis of cyclic polymers from alkynes. *Chem. Commun.* **2019**, *55*, 13697−13700.
(19) Hoskins, J. N.; Grayson, S. M. Cyclic polyesters: synthetic approaches and potential applications. *Polym. Chem.* **2011**, *2*, 289−299.
(20) Lee, S.; Kricheldorf, H. R. Polylactones. 35. Macrocyclic and stereoselective polymerization of β-D,L-butyrolactone with cyclic dibutyltin initiators. *Macromolecules* **1995**, *28*, 6718−6725.
(21) Nadif, S. S.; Kubo, T.; Gonsales, S. A.; VenkatRamani, S.; Ghiviriga, I.; Sumerlin, B. S.; Veige, A. S. Introducing "ynene" metathesis: ring-expansion metathesis polymerization leads to highly cis and syndiotactic cyclic polymers of norbornene. *J. Am. Chem. Soc.* **2016**, *138*, 6408−6411.
(22) Xia, Y.; Boydston, A. J.; Yao, Y.; Kornfield, J. A.; Gorodetskaya, I. A.; Spiess, H. W.; Grubbs, R. H. Ring-expansion metathesis polymerization: catalyst-dependent polymerization profiles. *J. Am. Chem. Soc.* **2009**, *131*, 2670−2677.
(23) Gonsales, S. A.; Kubo, T.; Flint, M. K.; Abboud, K. A.; Sumerlin, B. S.; Veige, A. S. Highly tactic cyclic polynorbornene: stereoselective ring expansion metathesis polymerization of norbornene catalyzed by a new tethered tungsten-alkylidene catalyst. *J. Am. Chem. Soc.* **2016**, *138*, 4996−4999.
(24) Niu, W. J.; Gonsales, S. A.; Kubo, T.; Bentz, K. C.; Pal, D.; Savin, D. A.; Sumerlin, B. S.; Veige, A. S. Polypropylene: now available without chain ends. *Chem* **2019**, *5*, 237−244.
(25) (a) Miao, Z.; Kubo, T.; Pal, D.; Sumerlin, B. S.; Veige, A. S. pH-responsive water-soluble cyclic polymer. *Macromolecules* **2019**, *52*, 6260−6265. (b) Miao, Z.; Pal, D.; Niu, W.; Kubo, T.; Sumerlin, B. S.; Veige, A. S. Cyclic poly(4-methyl-1-pentene): Efficient catalytic synthesis of a transparent cyclic polymer. *Macromolecules* **2020**, *53*, 7774−7782.
(26) Chang, Y. A.; Waymouth, R. M. Recent progress on the synthesis of cyclic polymers via ring-expansion strategies. *J. Polym. Sci., Part A: Polym. Chem.* **2017**, *55*, 2892−2902.
(27) Sheiko, S. S.; Sumerlin, B. S.; Matyjaszewski, K. Cylindrical molecular brushes: Synthesis, characterization, and properties. *Prog. Polym. Sci.* **2008**, *33*, 759−785.
(28) Zhang, K.; Lackey, M. A.; Wu, Y.; Tew, G. N. Universal cyclic polymer templates. *J. Am. Chem. Soc.* **2011**, *133*, 6906−6909.
(29) Schappacher, M.; Deffieux, A. Synthesis of macrocyclic copolymer brushes and their self-assembly into supramolecular tubes. *Science* **2008**, *319*, 1512−1515.
(30) Zhang, K.; Zha, Y.; Peng, B.; Chen, Y.; Tew, G. N. Metallo-supramolecular cyclic polymers. *J. Am. Chem. Soc.* **2013**, *135*, 15994−15997.
(31) Lahasky, S. H.; Serem, W. K.; Guo, L.; Garno, J. C.; Zhang, D. Synthesis and characterization of cyclic brush-like polymers by *N*-heterocyclic carbene-mediated zwitterionic polymerization of *N*-propargyl *N*-carboxyanhydride and the grafting-to approach. *Macromolecules* **2011**, *44*, 9063−9074.

(32) Xia, Y.; Boydston, A. J.; Grubbs, R. H. Synthesis and direct imaging of ultrahigh molecular weight cyclic brush polymers. *Angew. Chem., Int. Ed.* **2011**, *50*, 5882−5885.
(33) Boydston, A. J.; Holcombe, T. W.; Unruh, D. A.; Frechet, J. M. J.; Grubbs, R. H. A direct route to cyclic organic nanostructures via ring-expansion metathesis polymerization of a dendronized macromonomer. *J. Am. Chem. Soc.* **2009**, *131*, 5388−5389.
(34) Sheiko, S. S.; Sun, F. C.; Randall, A.; Shirvanyants, D.; Rubinstein, M.; Matyjaszewski, K.; et al. Adsorption-induced scission of carbon−carbon bonds. *Nature* **2006**, *440*, 191−194.
(35) Lebedeva, N. V.; Sun, F. C.; Lee, H.; Matyjaszewski, K.; Sheiko, S. S. "Fatal adsorption" of brushlike macromolecules: high sensitivity of C−C Bond cleavage rates to substrate surface energy. *J. Am. Chem. Soc.* **2008**, *130*, 4228−4229.
(36) Zhang, K.; Tew, G. N. Cyclic brush polymers by combining ring-expansion metathesis polymerization and the "grafting from" technique. *ACS Macro Lett.* **2012**, *1*, 574−579.
(37) Tu, X. Y.; Meng, C.; Zhang, X.-L.; Jin, M. G.; Zhang, X. S.; Zhao, X. Z.; Wang, Y. F.; Ma, L. W.; Wang, B. Y.; Liu, M. Z.; Wei, H. Fabrication of reduction-sensitive amphiphilic cyclic brush copolymer for controlled drug release. *Macromol. Biosci.* **2018**, *18*, No. 1800022.
(38) Wang, C. E.; Wei, H.; Tan, N.; Boydston, A. J.; Pun, S. H. Sunflower polymers for folate-mediated drug delivery. *Biomacromolecules* **2016**, *17*, 69−75.
(39) Tu, X. Y.; Meng, C.; Wang, Y. F.; Ma, L. W.; Wang, B. Y.; He, J. L.; Ni, P. H.; Ji, X. L.; Liu, M. Z.; Wei, H. Fabrication of thermosensitive cyclic brush copolymer with enhanced therapeutic efficacy for anticancer drug delivery. *Macromol. Rapid Commun.* **2018**, *39*, No. 1700744.
(40) Zhang, S.; Yin, L.; Zhang, W.; Zhang, Z.; Zhu, X. Synthesis of diverse cyclic-brush polymers with cyclic polystyrene as a universal template via a grafting-from approach. *Polym. Chem.* **2016**, *7*, 2112−2120.
(41) Wei, H.; Chu, D. S. H.; Zhao, J.; Pahang, J. A.; Pun, S. H. Synthesis and evaluation of cyclic cationic polymers for nucleic acid delivery. *ACS Macro Lett.* **2013**, *2*, 1047−1050.
(42) Fan, X.; Wang, G.; Huang, J. Synthesis of macrocyclic molecular brushes with amphiphilic block copolymers as side chains. *J. Polym. Sci., Part A: Polym. Chem.* **2011**, *49*, 1361−1367.
(43) McGowan, K. P.; O'Reilly, M. E.; Ghiviriga, I.; Abboud, K. A.; Veige, A. S. Compelling mechanistic data and identification of the active species in tungsten-catalyzed alkyne polymerizations: conversion of a trianionic pincer into a new *tetraanionic* pincer-type ligand. *Chem. Sci.* **2013**, *4*, 1145−1155.
(44) Mastrorilli, P.; Nobile, C. F.; Rizzuti, A.; Suranna, G. P.; Acierno, D.; Amendola, E. Polymerization of phenylacetylene and of *p*-tolylacetylene catalyzed by *β*-dioxygenato rhodium(I) complexes in homogeneous and heterogeneous phase. *J. Mol. Catal. A: Chem.* **2002**, *178*, 35−42.
(45) Trhlíková, O.; Zedník, J.; Balcar, H.; Brus, J.; Sedláček, J. [Rh(cycloolefin)(acac)] complexes as catalysts of polymerization of aryl- and alkylacetylenes: Influence of cycloolefin ligand and reaction conditions. *J. Mol. Catal. A: Chem.* **2013**, *378*, 57−66.
(46) Sarkar, S.; McGowan, K. P.; Kuppuswamy, S.; Ghiviriga, I.; Abboud, K. A.; Veige, A. S. An OCO^{3-} trianionic pincer tungsten (VI) alkylidyne: rational design of a highly active alkyne polymerization catalyst. *J. Am. Chem. Soc.* **2012**, *134*, 4509−4512.
(47) Sumerlin, B. S.; Neugebauer, D.; Matyjaszewski, K. Initiation efficiency in the synthesis of molecular brushes by grafting from via atom transfer radical polymerization. *Macromolecules* **2005**, *38*, 702−708.
(48) Neugebauer, D.; Sumerlin, B. S.; Matyjaszewski, K.; Goodhart, B.; Sheiko, S. S. How dense are cylindrical brushes grafted from a multifunctional macroinitiator? *Polymer* **2004**, *45*, 8173−8179.
(49) Carmean, R. N.; Becker, T. E.; Sims, M. B.; Sumerlin, B. S. Ultra-high molecular weights via aqueous reversible-deactivation radical polymerization. *Chem* **2017**, *2*, 93−101.
(50) Carmean, R. N.; Sims, M. B.; Figg, C. A.; Hurst, P. J.; Patterson, J. P.; Sumerlin, B. S. Ultra-high molecular weight hydrophobic acrylic and styrenic polymers through organic-phase photoiniferter-mediated polymerization. *ACS Macro Lett.* **2020**, *9*, 613−618.
(51) Schue, E.; Kopyshev, A.; Lutz, J.-F.; Börner, H. G. Molecular bottle brushes with positioned selenols: Extending the toolbox of oxidative single polymer chain folding with conformation analysis by atomic force microscopy. *J. Polym. Sci.* **2020**, *58*, 154−162.
(52) Daniel, W. F. M.; Burdyńska, J.; Vatankhah-Varnoosfaderani, M.; Matyjaszewski, K.; Paturej, J.; Rubinstein, M.; Dobrynin, A. V.; Sheiko, S. S. Solvent-free, supersoft and superelastic bottlebrush melts and networks. *Nat. Mater.* **2016**, *15*, 183−189.
(53) Mukherjee, S.; Xie, R.; Reynolds, V. G.; Matyjaszewski, K.; Uchiyama, T.; Levi, A. E.; Valois, E.; Wang, H.; Chabinyc, M. L.; Bates, C. M. Universal approach to photo-crosslink bottlebrush polymers. *Macromolecules* **2020**, *53*, 1090−1097.

https://dx.doi.org/10.1021/acs.macromol.0c01797
Macromolecules 2020, 53, 9717−9724